

**NEW MARINER 6 AND 7 MOSAICS OF MARS: CLUES ABOUT TIME VARIABLE SURFACE FEATURES.** J. L. Edmonds<sup>1</sup> and M. S. Robinson<sup>1</sup>, <sup>1</sup>Department of Geological Sciences, Northwestern University.

**Introduction:** Reprocessed far encounter data from Mariner 6 and 7 (1969) provide a valuable timestep with which to examine large scale surface processes on Mars. Although low resolution (20 km/pixel), the Mariner 6 and 7 far encounter images easily resolve large scale albedo features (>100 km). Planetary observers over the last century have tracked variations in size, shape, and location of albedo units. It is commonly assumed that these variations are due to eolian displacement of a layer of bright surface dust, possibly only  $\mu\text{m}$ 's thick, such that dark material beneath is revealed (e.g. [1], [2], [3], [4], [5]). Other mechanisms thought to be responsible for albedo region boundary movement are suspension of dust during saltation of coarser grains, and short distance displacement of these larger dark particles, usually in the context of wind streaks (e.g. [6], [3], [7], [8], [9], [10]). Comparison of Mariner 6 and 7 data with subsequent spacecraft data and earlier telescopic data is useful in tracking albedo unit variations over time and thus identifying mechanisms responsible for these variations. For example, comparing the size and location of albedo features in each data set with recorded dust storm occurrence [11] before the images were obtained allows for derivation of a cause-effect relationship between dust storms and albedo feature variations, as well as rates of atmospheric clearing.

**Data Processing:** We have recovered radiometrically calibrated Mariner 6 and 7 image data from 7-track tapes in order to aid our study and make these data readily available to the science community. No SPICE files were available for these images, so it was necessary to navigate them manually using spacecraft range to planet estimates [12], as well as tiepointing to a USGS Viking global basemap. Six Mariner 6 images and nine Mariner 7 images were tied directly to Viking images using control points such as craters, mountains and canyons. The remaining Mariner 6 (n=10) and Mariner 7 (n=15) images that were not tied directly to Viking were matched to each other using ground control points, and then tied to the Viking-controlled Mariner images. After several iterations, the control network solution for Mariner 6 had an average error of 0.9 pixel, with a maximum error of 1.7 pixels. The Mariner 7 control network solution had an average error of 1.0 pixel, with a maximum error of 1.9 pixels. The new camera angles were stored in the image labels, and the Mariner 6 and 7 images were reprojected into global maps for comparison with other global data sets. Photometric correction was applied to the images so that relative albedo values matched in the final mosaicked product. All pixels were normalized to standard lighting and viewing geometry (incidence angle =  $0^\circ$ , emission angle =  $0^\circ$ ) using a Minneart function with  $k = 0.7$  [13].

**Discussion:** Data sets used for comparison of albedo features included Viking MDIM, Hubble Space Telescope, and Mars Global Surveyor MOC. Additional analysis was done with Mariner 9, Viking IRTM, MOLA digital elevation model, and USGS Geologic Maps. Changes in large scale albedo features were recorded for each image mosaic. For example, Hyblaeus Chaos (Hy), centered at approximately  $24^\circ\text{N}$ ,  $238^\circ\text{W}$ , is an albedo feature that first appeared in Viking (Fig. 2), and is not seen in Mariner 6 and 7, Mariner 9, HST, or MOC. (The name of the feature is unclear; for the purposes of this abstract Hy will be used, taken from Figure 2 of [14].) The boundaries of Hy do not correspond with any topographic, geologic, or thermal inertia boundaries. For this reason, wind mechanisms that may be ascribed to many albedo feature variations (such as wind-swept highlands or cratered regions that trap dust) are not necessarily applicable to Hy, and there seems little reason for the preferential dust removal that uncovered this feature. Hy is particularly interesting because it does not correlate with a low thermal inertia region, as is typical with other low albedo units. This indicates that either the layer of high reflectance dust blanketing the rest of Elysium Planitia is very thin ( $\mu\text{m}$ - to mm-scale), or the dark grains of Hy are the same size as the surrounding bright grains. Another striking feature in the Mariner 7 mosaic is the latitudinal band of low albedo material in the Southern Hemisphere, which covers a much greater surface area in the Mariner 7 mosaic than in the Viking mosaic (Figs. 1, 2). In Mariner 7, the low albedo material extends to the ice cap, but in Viking, the low albedo material is bounded at approximately  $40^\circ\text{S}$  by intermediate albedo material. This is most likely because the Mariner 7 mosaic represents a period of time in which the planet was more clear of dust than during the Viking observations, which were shortly after two global dust storms. The appearance of Hy in Viking contradicts this reasoning: if the Mariner 7 images were acquired during a clear period, Hy should be visible in the Mariner 7 mosaic and obscured in the Viking mosaic. Another possibility is that dust storms transport a small amount of low albedo silt sized particles [9] in addition to bright dust, and this silt was deposited to form Hy after the 1977 dust storms. Large scale surface changes such as Hy and the southern dark band indicate significant mass transport that likely takes place during major dust storms. Weekly global mosaics using present Mars-orbiting spacecraft and HST would provide an opportunity to better track the intermediate steps of regional albedo changes and elucidate atmospheric clearing and large scale surface changes.

**References:** [1] Carr M. (1981) *The Surface of Mars*. [2] Pollack J. and Sagan C. (1967) *Icarus*, 6,

434-439. [3] Sagan C. et al. (1972) *Icarus*, 17, 346-372. [4] Chaikin A. et al. (1981) *Icarus*, 45, 167-178. [5] Cutts J. et al. (1971) *JGR*, 76, 343-356. [6] Thomas P. and Veverka J. (1986) *Icarus*, 66, 39-55. [7] Thomas P. et al. (1981) *Icarus*, 45, 124-153. [8] Thomas P. et al. (1984) *Icarus*, 60, 161-179. [9] Edgett K.

and Malin M. (2000) *JGR*, 105, 1623-1650. [10] Greeley R. et al. (1992) *Mars*, 686-729. [11] Martin L. and Zurek R. (1993) *JGR*, 98, 3221-3246. [12] Collins S. (1971) *The Mariner 6 and 7 Pictures of Mars*, NASA SP 263. [13] Thorpe T.E. (1973) *Icarus*, 20, 482-489. [14] Bell J. (1999) *Icarus*, 138, 25-35.

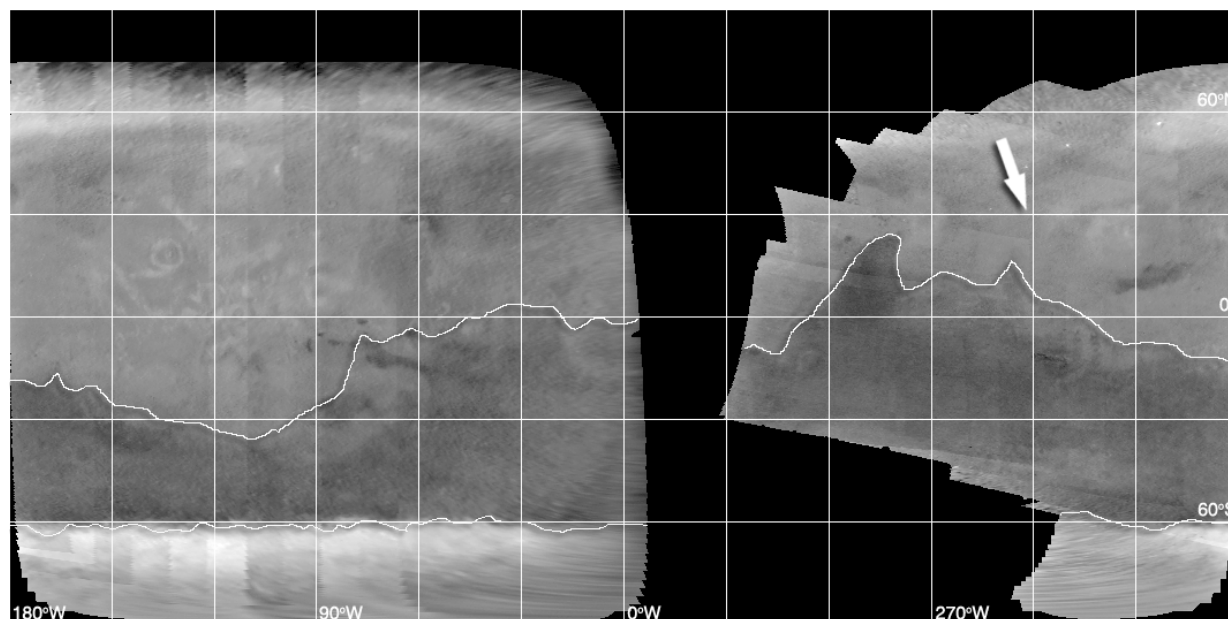


**Figure 1:** Newly reprocessed Mariner 7 image mosaic of Mars (simple cylindrical projection, 20 km/pixel, 24 images). The arrow points to where Hyblaeus Chaos appears in Viking (Fig. 2), and the thin white line bounds the low albedo southern band. The Mariner 6 mosaic covers a similar area, and the Mariner 6 images were acquired five days before the Mariner 7 images (<http://www.earth.northwestern.edu/research/robinson/mar67.html>).

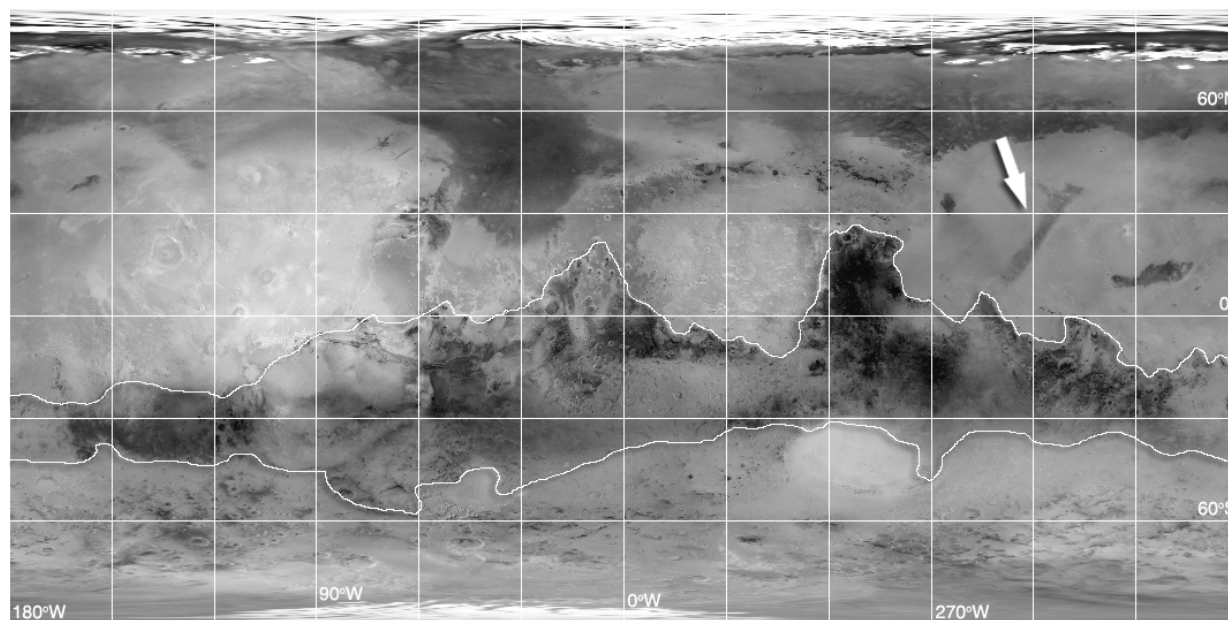


**Figure 2:** USGS Viking mosaic (simple cylindrical projection, 20 km/pixel). The arrow points to Hyblaeus Chaos, and the thin white line bounds the low albedo southern band, which covers much less surface area here than in Mariner 7.